ISSN 0023-1584, Kinetics and Catalysis, 2006, Vol. 47, No. 3, pp. 430–436. © MAIK "Nauka/Interperiodica" (Russia), 2006.
Original Russian Text © A.N. Salanov, A.I. Titkov, V.N. Bibin, 2006, published in Kinetika i Kataliz, 2006, Vol. 47, No. 3, pp. 438–445.

Mechanisms of Oxygen Adsorption and Desorption on Polycrystalline Palladium

A. N. Salanov, A. I. Titkov, and V. N. Bibin

Boreskov Institute of Catalysis, Siberian Division, Russian Academy of Sciences, Novosibirsk, 630090 Russia

Received November 12, 2004

Abstract—The adsorption and desorption of oxygen on a polycrystalline palladium (Pd(poly)) surface (10- to 100-μm crystallites; ~32% (100), ~18% (111), ~34% (311), and ~15% (331)) at $P_{O_2} \le 1.3 \times 10^{-5}$ Pa and T = 500–1300 K have been studied by TPD and mathematical modeling. The kinetics of O_2 adsorption and desorption on Pd(poly) are primarily governed by the formation and decomposition of oxygen adsorption structures on the (100) and (111) crystallite faces. The O_2 adsorption rate is constant at $\theta \le 0.15$–0.25 owing to the formation of the $p(2 \times 2)$ structure with an O_{ads}–surface bonding energy of D(Pd–O) = 364 kJ/mol on the (100) and (111) faces. The adsorption rate decreases with increasing coverage at $\theta \ge 0.15$–0.25 because of the growth, on the (100) face, of the $c(2 \times 2)$ structure, in which D(Pd–O) is reduced to 324 kJ/mol by lateral interactions in the adsorption layer. A high-temperature (~800 K) O_2 desorption peak is observed for $\theta \le 0.25$, which is due to O_2 desorption from a disordered adsorption layer according to a second-order rate law with an activation energy of E_{des} = 230 kJ/mol. A lower temperature (~700 K) O_2 desorption peak is observed for $\theta \ge 0.25$, which is due to O_2 released by the $c(2 \times 2)$ structure according to a first-order rate law with E_{des} = 150 kJ/mol. At $\theta \ge 0.25$, there are repulsive interactions between O_{ads} atoms on Pd(poly) (ε_{aa} = 5–10 kJ/mol).

DOI: 10.1134/S0023158406030153

Palladium is among the main components of automotive three-way catalysts [1, 2] and catalysts for complete methane oxidation in gas turbines [3] and for other important processes. Palladium is used in these catalysts because it is active both in the complete oxidation of hydrocarbons, CO, and H_2 and in NO reduction. The widespread employment of Pd in commercial catalysis has stimulated advanced instrumental investigation into the mechanisms of O_2, H_2, NO, CO, and CH_4 adsorption and desorption and into catalytic CO, H_2, and CH_4 oxidation and NO reduction on Pd single crystals. Special interest has been attracted by the interaction between oxygen and palladium, because the resulting Pd–O phases exert a significant effect on palladium-catalyzed oxidation reactions [3].

Oxygen chemisorption on Pd(poly) [4, 5], Pd(111) [6–10], Pd(100) [11–15], and Pd(110) [16–21] at low O_2 pressures ($\le 10^{-5}$ Pa) and T = 100–600 K has been studied by temperature-programmed desorption (TPD) [5–7, 9, 10, 12, 13, 15, 18, 21], low-energy electron diffraction (LEED) [6, 8, 10–17], scanning tunneling microscopy (STM) [10, 15, 19, 20], and high-resolution electron energy loss spectroscopy (HREELS) [8, 14]. The interaction between oxygen and palladium is governed by the Pd surface temperature and O_2 pressure. It has been demonstrated for Pd(poly) [5], Pd(111) [7–9], Pd(100) [14], and Pd(110) [16] by using HREELS and an isotopic tracer technique that O_2 undergoes molecular adsorption at $T \le 160$–200 K and dissociative adsorption at $T \ge 160$–200 K and that chemisorbed oxygen undergoes associative desorption at $T \ge 600$–650 K. At 300–400 K, O_2 is dissociatively chemisorbed by various palladium faces with a sticking coefficient of s_0 = 0.4–0.8. At the initial stages of adsorption, when the oxygen coverage of the surface (θ) is low, s is constant. This may be an indication of precursor-mediated adsorption [4, 6, 9, 12, 16]. At 600–900 K, chemisorbed oxygen undergoes associative desorption from various palladium faces. At $\theta \le 0.25$, O_2 desorption gives rise to a high-temperature TPD peak at ~800 K and is a second-order reaction, the activation energy of desorption being 218 kJ/mol for Pd(poly) [5] and 230 kJ/mol for Pd(111) [6]. At θ = 0.25–0.5, oxygen desorption is characterized by a lower temperature peak at ~700 K and by a reaction order close to unity [5, 10, 12, 13, 15]. It has been demonstrated by LEED and STM that, at $T \ge 300$–400 K, various adsorption structures form on the Pd(111) and Pd(100) surfaces upon dissociative O_2 adsorption [6, 8, 10–15]. For example, a $p(2 \times 2)$ structure, whose limiting coverage is θ = 0.25, forms on the Pd(111) surface at T = 300 K and θ = 0–0.25 [6, 8, 10]. At $\theta \ge 0.25$, a $(\sqrt{3} \times \sqrt{3})R30$ structure is observed, which is saturated at θ = 0.33 [6]. For Pd(100), a $p(2 \times 2)$ structure (θ = 0.25) forms at 200–400 K and θ = 0–0.25 and a $c(2 \times 2)$ structure (θ = 0.5) is observed at $\theta \ge 0.25$ [11–15]. The saturation of the chemisorbed oxygen layers on Pd(111) and Pd(100) is followed by the reconstruction of these faces yielding

oxide-like structures [10, 11, 13–15]. On Pd(110) at T = 200–400 K, mobile chemisorbed Pd atoms interact with O_2 molecules being chemisorbed to produce $c(2 \times 4)$ reconstructive chain structures of the added row type [17–21]. The –Pd–O–Pd– chains in these structures are aligned with the [110] direction and are regularly spaced in the [100] direction [19–21].

Although the interaction between O_2 and various palladium faces has been comprehensively studied by a variety of physical methods, the effect of the formation and decomposition of adsorbed oxygen structures on O_2 adsorption and desorption on palladium has not been understood. Here, we report the effect of the formation and decomposition of oxygen adsorption structures on the oxygen adsorption and desorption kinetics on various palladium faces as determined from structural data for the palladium surface, O_2 adsorption and desorption kinetics, and the results of simulation of adsorption and desorption on Pd(poly).

EXPERIMENTAL

Experiments were carried out in an LEED-240 ultrahigh-vaccum spectrometer (Varian), which was pumped with an ion pump down to a residual pressure of $1–2 \times 10^{-8}$ Pa). The spectrometer was equipped with an HCVA-850 AES analyzer (VG), a Q-7 quadrupole mass spectrometer (VG), and a catalytic chamber allowing the sample to be exposed to a wide range of O_2 pressures (10^{-5}–10^3 Pa) and temperatures (300–1600 K). The sample surface was examined by Auger electron spectroscopy (AES), and the amount of chemisorbed oxygen was determined by TPD. The sample was polycrystalline palladium (Pd(poly)) foil with dimensions of $10 \times 5 \times 0.1$ mm. Sample temperature was measured with a W–Re thermocouple (W–5% Re/W–20% Re) welded to the lateral surface of the sample. According to X-ray diffraction data, the surface of the initial sample was made up by (100), (111), and (110) faces, whose contributions were 34, 8, and 5%, respectively, and by (311) and (331) stepped surfaces, whose contributions were 44 and 9%, respectively. The only impurity in the initial palladium sample was carbon. Prior to surface analysis, carbon was removed from the surface by exposing the sample to oxygen at T = 500–600 K and P_{O_2} = 1 Pa in the spectrometer chamber followed by heating the sample to 1300 K in vacuo. The sample was considered to be carbon-free if the amount CO and CO_2 released in a TPD run was less than 1% of the amount of desorbed O_2. The recrystallization processes induced by the interaction between O_2 and palladium yields crystallites on the sample surface. Figure 1 shows SEM images of the recrystallized Pd(poly) surface obtained at different magnifications. The recrystallized surface consists of 10- to 100-μm crystallites. According to X-ray diffraction data, the crystallized foil surface was made up by (100) and (111) faces, whose contribution was ~32 and ~18%, respectively, and by (311) and (331) stepped surfaces (~34 and ~15%, respectively). After recrystallization the contribution from the (100) face was almost unchanged, while the contribution from the stepped surface (311) was smaller and the contribution from the (111) face was 10% larger. Apparently, the (311) surface consists largely of (111) oriented terraces. Thus, the recrystallized Pd(poly) surface is dominated by (100) and (111) faces (~32 and ~18%, respectively) and by the (311) stepped surface (~34%) consisting of (111) terraces. According to data obtained by photoemission of adsorbed xenon (PAX), the recrystallized Pd(poly) surface is 40% (100) and 60% (110) [5]. The experimental setup, sample preparation, and experimental procedure are detailed elsewhere [22].

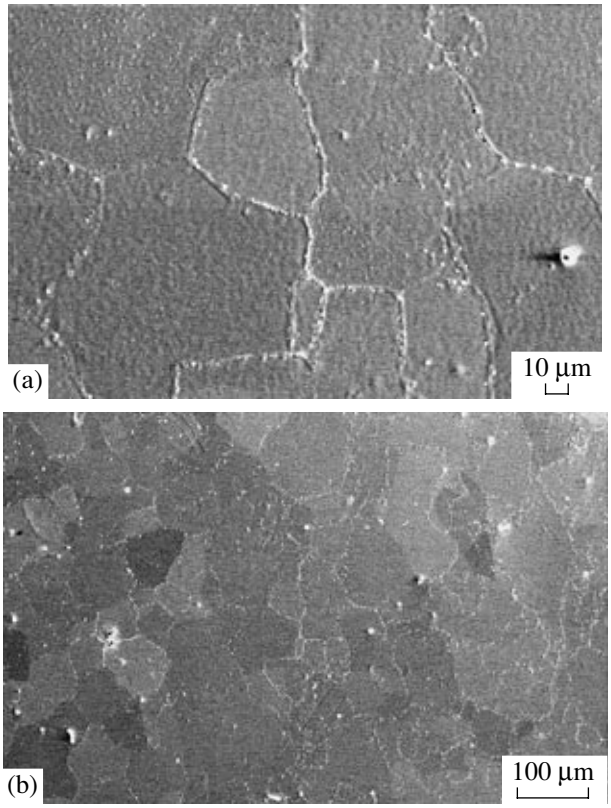

Fig. 1. SEM images of a recrystallized Pd(poly) surface at different magnifications. The size of the reference bar is (a) 10 and (b) 100 μm.

RESULTS AND DISCUSSION

Oxygen Chemisorption

Oxygen chemisorption onto recrystallized palladium foil (made up mainly of (100) and (111) crystallite faces) in the O_2 pressure range 1.3×10^{-7}–1.3×10^{-5} Pa at T = 500 K was studied by TPD. Figure 2 plots the chemisorbed-oxygen coverage of the Pd(poly) surface (θ) as a function of oxygen exposure doses (ε) at 500 K for three ε ranges: $\varepsilon \le 0.7$ L (Fig. 2a), $\varepsilon \le 2.0$ L

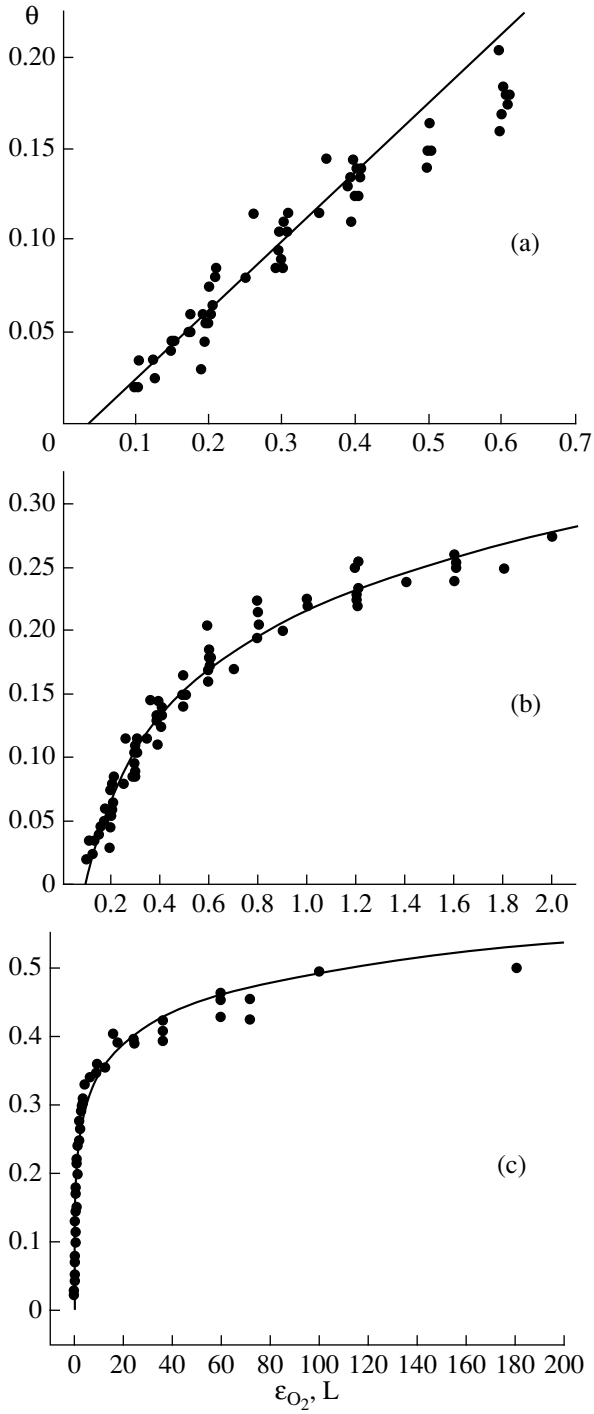

Fig. 2. Kinetics of oxygen adsorption on Pd(poly) at 500 K and $P_{O_2} = 1.3 \times 10^{-7}$–$1.3 \times 10^{-5}$ Pa for exposure dose (ε) ranges of (a) 0–0.7, (b) 0–2.0, and (c) 0–200 L.

(Fig. 2b), and ε ≤ 200 L (Fig. 2c) (1 L = 10^{-6} Torr s). The amount of chemisorbed oxygen was derived from TPD spectra. Saturating the Pd(100) and Pd(111) faces with oxygen yields $c(2 \times 2)$ and $p(2 \times 2)$ adsorption structures with θ = 0.5 and 0.25, respectively [6, 8, 10–15]. Therefore, it can be assumed that, the saturation of the Pd(poly) surface with oxygen (ε = 100–200 L) will result in a θ close to 0.5. For this reason, the amount of chemisorbed oxygen was determined from the O_2 TPD spectrum for ε = 180 L under the assumption that θ = 0.5. It is clear from Fig. 2 that the θ(ε) dependence changes significantly as θ increases. At the initial stages of adsorption, at ε = 0–0.4 L (Fig. 2a), θ gradually increases to 0.15 and the experimental data points fall on a straight line, indicating a constant adsorption rate ($s_0 = 0.7$ at these θ values). At 300–400 K, O_2 chemisorption on various palladium specimens is characterized by a sticking coefficient of $s_0 = 0.4$–0.8, which is again constant at the initial stages of adsorption [4, 6, 9, 12, 16]. As ε is increased to 2.0 L at 500 K, θ grows to 0.25 (Fig. 2b). As ε is further increased to 200 L, θ grows to 0.5 (Fig. 2c) and the experimental data points make up a logarithmic curve. Since the Pd(poly) surface consists largely of (100) and (111) faces (~32 and ~18%, respectively) and the (311) stepped surface (~34%), it is believed that the specific kinetic features of O_2 adsorption on Pd(poly) are mainly due to O_2 chemisorption on the (100) and (111) faces.

LEED studies of O_2 chemisorption on Pd(100) have demonstrated that $p(2 \times 2)$ islands form and gradually grow at the initial (θ ≥ 0.25) stages of chemisorption at $T \le 400$ K and, at θ ≤ 0.25, $c(2 \times 2)$ islands with a denser structure appear in the $p(2 \times 2)$ adsorption layer [11–13]. A Monte Carlo simulation of dissociative O_2 chemisorption on the (100) surface with a square lattice of adsorption sites, including direct and indirect adsorption mechanisms, has provided a description for the nucleation and growth of the adsorption structures $p(2 \times 2)$ and $c(2 \times 2)$ at θ ≤ 0.25 and 0.25–0.50, respectively [23, 24]. By direct adsorption, we mean the following mechanism: an O_2 molecule collides against a vacant adsorption site, overcomes the direct-adsorption activation barrier E_{dir}, dissociates, and is chemisorbed (generating adsorption islands). The oxygen atoms first occupy the nearest neighbor (NN) adsorption sites. Next, because of the strong repulsion between the atoms, one of them jumps to a third nearest adsorption site (3NN). Indirect adsorption (the growth of adsorption islands) takes place as follows: an O_2 molecule collides against an occupied adsorption site, is captured to pass into the precursor state, migrates over occupied adsorption sites, overcomes the indirect-adsorption barrier E_{ind}, and undergoes dissociative chemisorption at the island boundary, thus enlarging the island.

Using this chemisorption model [23, 24], we simulated, by the Monte Carlo method, the dissociative chemisorption of O_2 on the (100) surface to elucidate the roles of direct and indirect adsorption in the kinetics of O_2 chemisorption on palladium. We found that, at $E_{dir}/E_{ind} = 7$–8, direct adsorption dominates over indirect adsorption at θ ≤ 0.08–0.10 and the reverse situation is observed at θ ≥ 0.08–0.10. Figure 3 illustrates the dependence of the O_2 sticking coefficient on θ for direct adsorption (s_{dir}, curve *1*), indirect adsorption (s_{ind}, curve *2*), and both mechanisms taking place

simultaneously ($s = s_{dir} + s_{ind}$, curve *3*). The $s(\theta)$ relationships were established by simulating O_2 adsorption with E_{dir} = 7 kJ/mol and E_{ind} = 1 kJ/mol. At the early stages of adsorption, s_{dir} (curve *1*) is well above s_{ind} (curve *2*); however, s_{dir} decreases and s_{ind} increases in the course of adsorption. At θ = 0.08–0.10, the sticking coefficients are similar; at $\theta \geq$ 0.08–0.10, s_{ind} exceeds s_{dir}. As a consequence, s is invariable at $\theta \leq$ 0.08–0.10 and gradually decreases with increasing coverage at $\theta \geq$ 0.08–0.10. Therefore, the invariable rate of O_2 adsorption on Pd(poly) at $\theta \leq 0.15$ (Fig. 2a) may be due to the gradual changes in the contributions from the direct and indirect adsorption mechanisms into the oxygen buildup on the surface. At the early stages of adsorption (at $\theta \leq 0.15$), the rate of direct adsorption gradually decreases because it is proportional to the decreasing free surface fraction. As this takes place, the rate of indirect adsorption increases, because, at the early stages of adsorption, before the merging of $p(2 \times 2)$ islands, it is proportional to the increasing surface area occupied by adsorption islands. Thus, early in the adsorption process, when the surface coverage is low ($\theta \leq 0.15$), the observed adsorption rate is constant because the decrease in the rate of direct adsorption is compensated for by an increase in the rate of indirect adsorption (Fig. 2a). A constant O_2 adsorption rate at low θ values has already been observed for Pd(poly) [4], Pd(111) [6, 9], and Pd(100) [12, 16]. As the surface coverage increases further (at $\theta \geq$ 0.15–0.20), the adsorption rate decreases markedly (Fig. 2b). This may be due to the appearance of $c(2 \times 2)$ islands with a denser structure in the saturated adsorption layer $p(2 \times 2)$. These $c(2 \times 2)$ islands form mainly by the merging of antiphase $p(2 \times 2)$ islands and grow owing to the indirect dissociative adsorption of O_2 molecules [23]. In the $c(2 \times 2)$ structure, the chemisorbed oxygen atoms occupy the nearest diagonal adsorption sites (2NN). The atoms occupying these sites experience lateral repulsion. This interaction diminishes the M–O bond energy and, accordingly, increases the activation energy of the dissociative chemisorption of O_2 molecules on the vacant neighbor sites 2NN, thereby decreasing the adsorption rate [23]. Thus, at low oxygen coverages of the Pd(poly) surface ($\theta \leq 0.15$), the constant O_2 adsorption rate is due to the formation of the adsorption structure $p(2 \times 2)$ on the (100) and (111) faces. The dramatic fall of the O_2 adsorption rate at $\theta \geq$ 0.15 is due to the formation of the adsorption structure $c(2 \times 2)$ on the (100) face.

Desorption of Chemisorbed Oxygen

The thermal desorption of O_2 from Pd(poly) was studied at T = 500–1300 K over the heating rate (β) range 1–90 K/s. Figure 4a shows the oxygen TPD spectra recorded at β = 10 K/s after O_2 adsorption on Pd(poly) at T = 500 K, $P_{O_2} = 2.7 \times 10^{-6} - 2.7 \times 10^{-5}$ Pa, and ε = 0.2–180 L. Spectrum *10* (Fig. 4a), which was recorded while heating the saturated layer of adsorbed oxygen (ε = 180 L), is taken to correspond to θ = 0.5 for the reason that the sample surface consists mainly of (100), (111), and (311) faces (~32, ~18, and ~34%, respectively) and the saturation of the (100) and (111) faces with oxygen yields the adsorption structures $c(2 \times 2)$ and $p(2 \times 2)$ with θ = 0.50 and 0.25, respectively [6, 8, 10–15]. As θ increases from 0.06 to 0.30, the desorption peak gradually shifts from 875 to 800 K (Fig. 4a, curves *1–6*). This may be evidence that O_2 desorption obeys a second-order rate law. It has already been reported that the TPD peak in O_2 desorption from Pd(poly) [5], Pd(111) [10], and Pd(100) [12, 13, 15] at $\theta \leq 0.25$ shifts from 900 to 800 K as the surface coverage increases. It is believed that this shift is due to the second-order desorption of oxygen from a disordered adsorption layer [5, 10, 12, 13, 15]. As the oxygen coverage of the Pd(poly) surface increases, a lower temperature (T ~ 700 K) state appears at θ > 0.23–0.30 (Fig. 4a, curves *5–8*). $c(2 \times 2)$ islands, in which chemisorbed oxygen atoms occupy 2NN sites in the $p(2 \times 2)$ adsorption layer, form on the Pd(100) surface at $\theta \geq$ 0.20–0.25 [11–13]. The energy of the bond between such an atom and the surface is reduced by lateral interatomic repulsion. As a consequence, oxygen is desorbed at a lower temperature and the TPD spectrum indicates a lower temperature state (T ~ 700 K) [13]. In order to elucidate the effect of the repulsive interactions in the adsorption layer on O_2 desorption from Pd(poly), we simulated O_2 desorption with allowance made for lateral repulsion between nearest-neighbor adsorbed atoms (ε_{aa}). Figure 4b shows the TPD spectra calculated using the model presented in [26]. Clearly, at ε_{aa} = 5 kJ/mol and E_{des} = 230 kJ/mol, the calculated and observed spectra are in agreement. Since the adsorption layer on the (100) surface is saturated at θ = 0.50 [12–15],

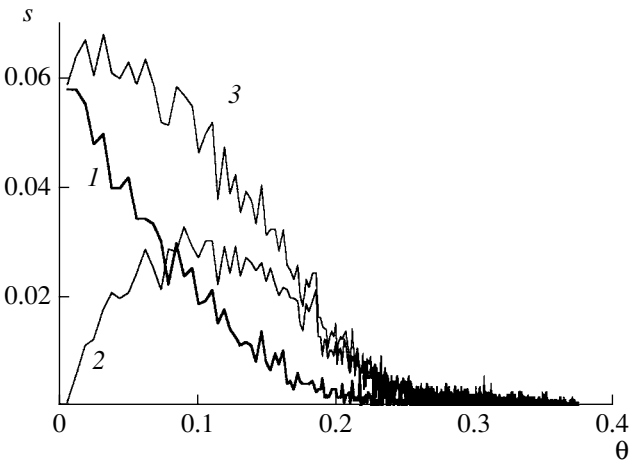

Fig. 3. O_2 sticking coefficient (s) versus the oxygen coverage of the surface (θ) for (*1*) direct adsorption, (*2*) indirect adsorption, and (*3*) both mechanisms taking place simultaneously, as calculated through the Monte Carlo simulation of dissociative O_2 chemisorption on the (100) surface.

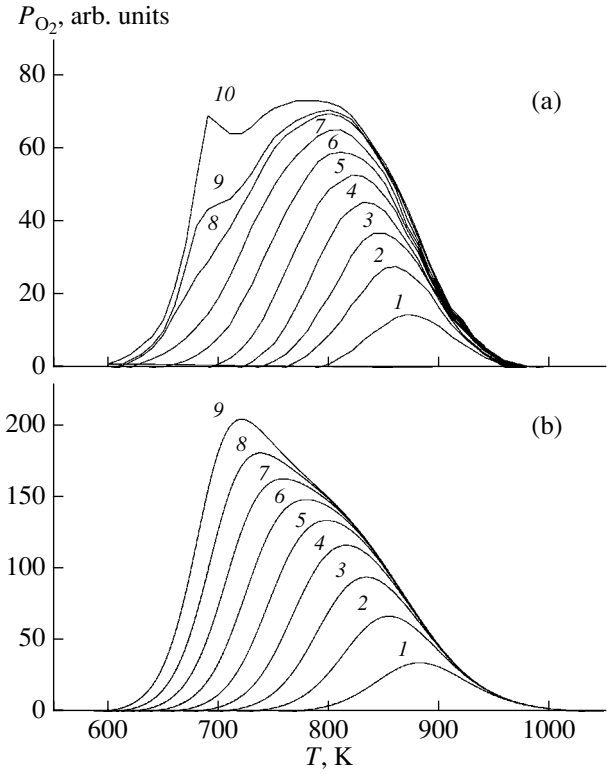

Fig. 4. (a) Oxygen TPD spectra obtained at β = 10 K/s for O_2 adsorbed on Pd(poly) at 500 K and $P_{O_2} = 2.7 \times 10^{-6} - 2.7 \times 10^{-5}$ Pa; the exposure dose is (*1*) 0.2, (*2*) 0.3, (*3*) 0.4, (*4*) 0.6, (*5*) 1.2, (*6*) 3, (*7*) 12, (*8*) 36, (*9*) 72, and (*10*) 180 L; the corresponding θ values are (*1*) 0.06, (*2*) 0.10, (*3*) 0.15, (*4*) 0.19, (*5*) 0.23, (*6*) 0.30, (*7*) 0.35, (*8*) 0.40, (*9*) 0.43, and (*10*) 0.50. (b) The same spectra calculated using a model taking into account lateral interactions [26] for E_{des} = 230 kJ/mol, $k_0 = 0.2$ cm^2/s, and $\varepsilon_{aa} = 5$ kJ/mol; θ = (*1*) 0.05, (*2*) 0.10, (*3*) 0.15, (*4*) 0.20, (*5*) 0.25, (*6*) 0.30, (*7*) 0.35, (*8*) 0.45, and (*9*) 0.50.

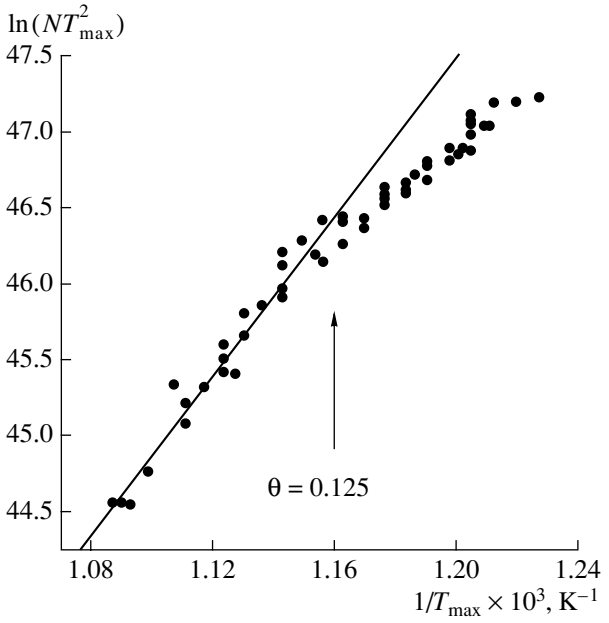

Fig. 5. Plot of $\ln(NT_{max}^2)$ versus $1/T_{max}$ derived from O_2 TPD data for Pd(poly) (points). The straight line represents the best fit for the experimental data for θ ≤ 0.125.

we will assume in simulating O_2 desorption that the saturated adsorption layer is characterized by θ = 0.50. At θ ≤ 0.25–0.30, the desorption peak shifts to lower temperatures, suggesting that oxygen desorption obeys a second-order rate law (Fig, 4b, curves *1–5*). The TPD spectra for θ ≥ 0.25–0.30 indicate a lower temperature state at T ~ 700 K (Fig. 4b, curves *6–9*). The thermal desorption of O_2 from Pd(100) at θ ≤ 0.45 has been successfully simulated under the assumption that there is repulsive interaction with an energy of 3.3 kJ/mol between nearest-neighbor chemisorbed atoms [13]. Therefore, in the O_2 TPD spectra for Pd(poly), the high-temperature (~800 K) peak for θ ≤ 0.25 is due to O_2 desorption from a disordered adsorption layer and the lower temperature (~700 K) peak for θ = 0.25–0.50 is due to O_2 released by the adsorption structure $c(2 \times 2)$.

The activation energy of O_2 desorption (E_{des}) and the preexponential factor (k_0) were determined for low oxygen coverages of the Pd(poly) surface (θ ≤ 0.25) from the Redhead equation for second-order desorption: $E_{des}/RT_{max}^2 = Nk_0/\beta \times \exp(-E_{des}/RT_{max})$ [25]. Here, T_{max} is the desorption peak temperature at a given θ, $N = \theta N_0$ is the concentration of chemisorbed oxygen, and $N_0 = 1.33 \times 10^{15}$ atoms/cm^2 is the density of Pd atoms on the Pd(100) surface. Figure 5 plots $\ln(NT_{max}^2)$ versus $1/T_{max}$. At low $1/T_{max}$ values of 0.00108 to 0.00116 and, accordingly, θ ≤ 0.125, the data points fall on a straight line. The slope of this line gives E_{des} = 218 kJ/mol, and the $\ln(NT_{max}^2)$ intercept leads to k_0 = 0.027 cm^2/s. According to earlier reports on O_2 desorption, E_{des} = 218 kJ/mol for Pd(poly) [5] and E_{des} = 230 kJ/mol for Pd(111) [6]. Furthermore, coverage-dependent E_{des} data for Pd(poly) have been derived from O_2 TPD spectra by the Habenschaden–Kuppers (H–K) method [27] and the heating rate (β) variation method. Figure 6 plots the E_{des} versus θ curves obtained by the H–K and β variation methods. The H–K method was used to derive E_{des} at a given coverage from the ln$P$ versus $1/T$ dependence for initial portions of TPD curves, at a coverage differing by at most 5% from its initial value (p is the relative desorption intensity at a given T). At low coverages (θ ≤ 0.25), E_{des} ~ 240 kJ/mol. As θ increases from 0.25 to 0.50, E_{des} gradually decreases to 140–150 kJ/mol. As θ increases from 0.5 to 1.0, E_{des} remains invariable (Fig. 6, points *1*). A similar E_{des} versus θ plot was derived by the H–K method from O_2 TPD data for Pd(poly) in an earlier study [5]:

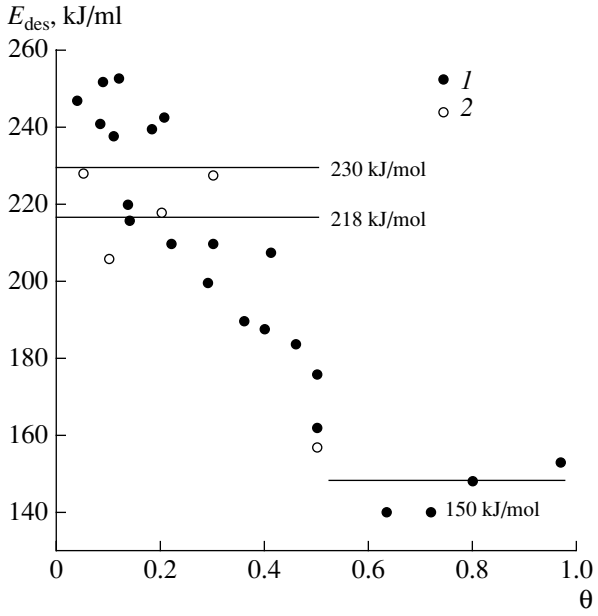

Fig. 6. (*1*) Activation energy of O_2 desorption from Pd(poly) as a function of surface coverage derived from initial porttions of TPD (ln P versus $1/T$) curves by the H–K method [27]. (*2*) The same derived from the $\ln(T_{max}^2/\beta)$ versus $1/T_{max}$ dependence [25] by varying the heating rate between 1 and 90 K/s. E_{des} = 230 kJ/mol is the mean activation energy for $\theta \le 0.25$, E_{des} = 218 kJ/mol is the activation energy derived from the $\ln(NT_{max}^2)$ versus $1/T_{max}$ dependence for $\theta \le 0.125$, and E_{des} = 150 kJ/mol is the mean activation energy for $\theta \ge 0.50$.

E_{des} ~ 218 kJ/mol for $\theta \le 0.10$ and E_{des} = 150–160 kJ/mol for $\theta \ge 0.10$. Varying the heating rate shifts the desorption peak along the temperature axis [25]. Varying the heating rate at a fixed coverage, it is possible to derive E_{des} at this θ from $T_{max}(\beta)$ and $\ln(T_{max}^2/\beta)$ versus $1/T_{max}$ data. Figure 6 (points *2*) plots θ-dependent E_{des} data obtained by varying β from 1 to 90 K/s. At low coverages ($\theta \le 0.3$), E_{des} has a constant value of ~220 kJ/mol. As θ increases above 0.30, E_{des} falls to ~150 kJ/mol. Clearly, these data are similar to the data obtained by the H–K method (points *1*). Applying the Redhead equation [25] to these E_{des} data, we determined the mean value of the preexponential factor for O_2 desorption: $k_0 = 0.2$ cm^2/s. The theoretical estimate of k_0 for associative desorption is 10^{-4}–10^4 cm^2/s [28]. The E_{des} data for O_2 desorption from Pd(poly) were used to derive the chemisorbed oxygen–palladium bonding energy (D(Pd–O)) from the equation $2D(\text{Pd–O}) = D(\text{O–O}) + q$, where D(O–O) is the dissociation energy of the O_2 molecule (498 kJ/mol) and q is the heat of adsorption of O_2. Since $q = E_{des} - E_a$ and the activation energy of O_2 chemisorption (E_a) is low (<10 kJ/mol), it can be assumed that $q \sim E_{des}$ and, therefore, D(Pd–O) can be derived from E_{des}. At low oxygen coverages of the Pd(poly) surface ($\theta \le 0.25$), E_{des} has a nearly constant value of ~230 kJ/mol. Hence, for these θ values, we obtain D(Pd–O) ~364 kJ/mol. At $\theta \ge 0.25$, E_{des} gradually decreases to 150 kJ/mol. Hence, for this θ range, D(Pd–O) ~ 324 kJ/mol. From the q values for $\theta \sim 0$ (q_0) and $\theta \sim 0.5$ ($q_{0.5}$), it is possible to derive the energy of lateral repulsion between chemisorbed atoms. For the lateral surrounding of a chemisorbing molecule at $\theta = 0$ and 0.5, we obtain $\varepsilon_{aa} = (q_0 - q_{0.5})/8 =$ 10 kJ/mol. Therefore, the fact that E_{des} for O_2 desorption from Pd(poly) is nearly invariable at $\theta \le 0.25$ indicates that the adsorbed atoms–surface bonding energy is constant (D(Pd–O) = 364 kJ/mol). The constancy of D(Pd–O) at these θ values is evidence of the absence of lateral interactions between O_{ads} atoms. The dramatic fall of E_{des} to 150 kJ/mol at $\theta \sim 0.25$ indicates that D(Pd–O) decreases to 324 kJ/mol. This decrease in D(Pd–O) is evidence that repulsive interactions characterized by $\varepsilon_{aa} = 10$ kJ/mol at this θ appear in the adsorbed layer. This obviously suggests the formation of the adsorption structure $c(2 \times 2)$, since the adsorbate–surface bonding energy in this structure is markedly reduced by the lateral interactions between O_{ads} atoms.

CONCLUSIONS

The chemisorption of O_2 on Pd(poly) at T = 500 K proceeds at a constant rate of $s_0 = 0.7$ at $\theta \le 0.15$ and at a markedly decreasing rate at $\theta \ge 0.15$. It was found by the Monte Carlo simulation of the dissociative chemisorption of O_2 on the (100) surface that the constancy of the adsorption rate at $\theta \le 0.15$ can be due to a gradual decrease in the nucleation rate of $p(2 \times 2)$ adsorption islands compensated for by an increase in the growth rate of these islands on the (100) and (111) crystallite faces. The decrease in the adsorption rate at $\theta \ge 0.15$–0.20 can be due to a gradual nucleation and growth of $c(2 \times 2)$ islands in the saturated adsorption layer $p(2 \times 2)$ on the (100) faces, because the lateral repulsion between O_{ads} atoms in these islands diminishes the O_{ads}–surface bonding energy (D(Pd–O)) and, accordingly, raises the activation energy of adsorption [23]. Oxygen desorbed from Pd(poly) at $\theta \le 0.25$ gives rise to a TPD peak at ~800 K, which is due second-order O_2 desorption from a disordered adsorption layer (E_{des} = 230 kJ/mol). At $\theta \le 0.25$, the O_{ads}–surface bonding energy is 364 kJ/mol. The desorption of O_2 from Pd(poly) at $\theta \ge 0.25$ is manifested as a TPD peak at ~700 K, which is due to the first-order decomposition of the adsorption layer $c(2 \times 2)$ (E_{des} = 150 kJ/mol). At $\theta \ge 0.25$, D(Pd–O) gradually decreases from 364 to 324 kJ/mol as θ increases, indicating that lateral interactions with ε_{aa} = 10 kJ/mol come into play in the adsorption layer. The simulation of associative O_2 desorption from Pd(poly) with allowance made for O_{ads} repulsion with ε_{aa} = 5 kJ/mol, E_{des} = 230 kJ/mol, and $k_0 = 0.2$ cm^2/s accounts for the high-temperature

(~800 K) O_2 desorption peak observed for $\theta \le 0.25$ and for the lower temperature (~700 K) peak observed for $\theta = 0.25$–0.50. The simulated O_2 TPD spectra and the data derived from the dependence of E_{des} on θ for Pd(poly) indicate that, at $\theta \ge 0.25$, there are lateral repulsive interactions between chemisorbed O atoms in the oxygen layer adsorbed on Pd(poly) (ε_{aa} = 5–10 kJ/mol).

Thus, the kinetics of O_2 adsorption and desorption on Pd(poly) are mainly governed by the formation and decomposition of oxygen adsorption structures on the (100) and (111) crystallite faces on the sample surface. At low coverages of $\theta \le 0.15$–0.25, O_2 is adsorbed by Pd(poly) at a constant rate ($s_0 = 0.7$) owing to the formation of the $p(2 \times 2)$ structure on the (100) and (111) faces and is desorbed from a disordered adsorption layer according to a second-order rate law with E_{des} = 230 kJ/mol, giving rise to a TPD peak at ~800 K. At $\theta \ge 0.15$–0.25, O_2 is desorbed at a lower rate because of the formation of the $c(2 \times 2)$ structure on the (100) surface and is desorbed owing to the decomposition of this structure according to a first-order law with E_{des} = 150 kJ/mol, giving rise to a TPD peak at a lower temperature of ~700 K.

ACKNOWLEDGMENTS

This work was supported by the Russian Foundation for Basic Research, project no. 03-03-33177. The authors are grateful to S.V. Bogdanov for X-ray crystallographic characterization of the polycrystalline palladium surface.

REFERENCES

1. Heck, R.M. and Farrauto, R.J., *Catalytic Air Pollution Control: Commercial Technology*, New York: Van Nostrand, 1995, p. 102.
2. Nieuwenhuys, B.E., *Adv. Catal.*, 1999, vol. 44, p. 259.
3. Ciuparu, D., Lyubovsky, M.R., Altman, E., Pfefferle, L.D., and Datye, A., *Catal. Rev.*, 2002, vol. 44, p. 593.
4. Matsushima, T. and White, J.M., *Surf. Sci.*, 1977, vol. 67, p. 122.
5. Milun, M. and Pervan, P., *Surf. Sci.*, 1989, vol. 218, p. 363.
6. Conrad, H., Ertl, G., Kuppers, G., and Latta, E.E., *Surf. Sci.*, 1977, vol. 65, p. 245.
7. Matsushima, T., *Surf. Sci.*, 1985, vol. 157, p. 297.
8. Imbihl, R. and Demuth, J.E., *Surf. Sci.*, 1986, vol. 173, p. 395.
9. Guo, X., Hoffman, A., and Yates, J.T., Jr., *J. Chem. Phys.*, 1989, vol. 90, p. 5787.
10. Zheng, G. and Altman, E.I., *Surf. Sci.*, 2000, vol. 462, p. 151.
11. Orent, T.W. and Bader, S.D., *Surf. Sci.*, 1982, vol. 115, p. 323.
12. Stuve, E.M., Madix, R.J., and Brundle, C.R., *Surf. Sci.*, 1984, vol. 146, p. 155.
13. Chang, S.L. and Thiel, P.A., *J. Chem. Phys.*, 1988, vol. 88, p. 2071.
14. Simmons, G.W., Wang, Y-N., Marcos, J., and Klier, K., *J. Phys. Chem.*, 1991, vol. 95, p. 4522.
15. Zheng, G. and Altman, E.I., *Surf. Sci.*, 2002, vol. 504, p. 253.
16. Goschnick, J., Wolf, M., Grunze, M., Unertl, W.N., Block, J.H., and Loboda-Cackovic, J., *Surf. Sci.*, 1986, vol. 178, p. 831.
17. He, J.-W., Memmert, U., Griffiths, K., and Norton, P.R., *J. Chem. Phys.*, 1989, vol. 90, p. 5082.
18. Jones, I.Z., Bennett, R.A., and Bowker, M., *Surf. Sci.*, 1999, vol. 439, p. 235.
19. Bennett, R.A., Poulston, S., Jones, I.Z., and Bowker, M., *Surf. Sci.*, 1998, vol. 401, p. 72.
20. Yagi, K. and Fukutani, H., *Surf. Sci.*, 1998, vols. 412–413, p. 489.
21. Yagi, K., Sekiba, D., and Fukutani, H., *Surf. Sci.*, 1999, vol. 442, p. 307.
22. Salanov, A.N. and Savchenko, V.I., *Kinet. Katal.*, 1992, vol. 33, no. 2, p. 381.
23. Salanov, A.N. and Bibin, V.N., *Surf. Sci.*, 1999, vol. 441, p. 399.
24. Salanov, A.N., Bibin, V.N., and Yakushko, V.T., *J. Mol. Catal. A: Chem.*, 2000, vol. 158, p. 367.
25. Redhead, P.A., *Vacuum*, 1962, vol. 12, p. 203.
26. Zhdanov, V.P., *Surf. Sci.*, 1981, vol. 111, p. 63.
27. Habenschaden, E. and Kuppers, J., *Surf. Sci.*, 1984, vol. 138, p. L147.
28. Zhdanov, V.P., *Surf. Sci. Rep.*, 1991, vol. 12, p. 183.